

ORIGINAL RESEARCH

Glycoursodeoxycholic Acid Ameliorates Atherosclerosis and Alters Gut Microbiota in Apolipoprotein E–Deficient Mice

Kan Huang , MD*; Chenshu Liu, MD*; Meixiu Peng, MSc; Qiao Su, BSc; Ruiming Liu, PHD; Zeling Guo, MB; Sifan Chen, MD, PHD; Zilun Li, MD, PHD; Guangqi Chang , MD

BACKGROUND: Although glycoursodeoxycholic acid (GUDCA) has been associated with the improvement of metabolic disorders, its effect on atherosclerosis remains elusive. This study aimed to investigate the role of GUDCA in the development of atherosclerosis and its potential mechanisms.

METHODS AND RESULTS: Human THP-1 macrophages were used to investigate the effect of GUDCA on oxidized low-density lipoprotein–induced foam cell formation in vitro. We found that GUDCA downregulated scavenger receptor A1 mRNA expression, reduced oxidized low-density lipoprotein uptake, and inhibited macrophage foam cell formation. In an in vivo study, apolipoprotein E–deficient mice were fed a Western diet for 10 weeks to induce atherosclerosis, and then were gavaged once daily with or without GUDCA for 18 weeks. Parameters of systemic metabolism and atherosclerosis were detected. We found that GUDCA improved cholesterol homeostasis and protected against atherosclerosis progression as evidenced by reduced plaque area along with lipid deposition, ameliorated local chronic inflammation, and elevated plaque stability. In addition, 16S rDNA sequencing showed that GUDCA administration partially normalized the Western diet–associated gut microbiota dysbiosis. Interestingly, the changes of bacterial genera (*Alloprevotella*, *Parabacteroides*, *Turicibacter*, and *Alistipes*) modulated by GUDCA were correlated with the plaque area in mice aortas.

CONCLUSIONS: Our study for the first time indicates that GUDCA attenuates the development of atherosclerosis, probably attributable to the inhibition of foam cell formation, maintenance of cholesterol homeostasis, and modulation of gut microbiota.

Key Words: atherosclerosis ■ cholesterol homeostasis ■ foam cell ■ glycoursodeoxycholic acid ■ gut microbiota

Atherosclerosis is the vicious culprit behind most cardiovascular disease (CVD), which persists as the leading cause of adult morbidity and mortality worldwide.¹ Atherosclerosis is recognized as a consequence of metabolic disorders, and cholesterol imbalance is associated with the development of atherosclerosis.^{2–4} While current treatment with cholesterol-lowering compounds such as statins have prevented nearly half of CVD events, the substantial

risk of CVD events remains.^{5,6} To date, the mechanism of atherosclerosis remains largely unknown.

Microbiota play an important role in regulation of host physiology.^{7,8} Most recently, increasing evidence suggests that dysbiosis of gut microbiota is closely related to the development of atherosclerosis. For example, the composition and relative abundances of gut microbiota in patients with atherosclerotic cardiovascular disease (ASCVD) differ from health controls.⁹ Oral

Correspondence to: Guangqi Chang, MD, Division of Vascular Surgery, National-Guangdong Joint Engineering Laboratory for Diagnosis and Treatment of Vascular Diseases, The First Affiliated Hospital of Sun Yat-sen University, NO.58, Zhongshan 2nd Road, Guangzhou 510080, Guangdong, P.R. China. E-mail: changgq@mail.sysu.edu.cn or Zilun Li, MD, PHD, Division of Vascular Surgery, National-Guangdong Joint Engineering Laboratory for Diagnosis and Treatment of Vascular Diseases, The First Affiliated Hospital of Sun Yat-sen University, NO.58, Zhongshan 2nd Road, Guangzhou 510080, Guangdong, P.R. China. E-mail: lizilun@mail.sysu.edu.cn.

*K. Huang and C. Liu contributed equally.

Supplementary Material for this article is available at <https://www.ahajournals.org/doi/suppl/10.1161/JAHA.120.019820>

For Sources of Funding and Disclosures, see page 13.

© 2021 The Authors. Published on behalf of the American Heart Association, Inc., by Wiley. This is an open access article under the terms of the Creative Commons Attribution-NonCommercial-NoDerivs License, which permits use and distribution in any medium, provided the original work is properly cited, the use is non-commercial and no modifications or adaptations are made.

JAHA is available at: www.ahajournals.org/journal/jaha

CLINICAL PERSPECTIVE

What Is New?

- Glycoursodeoxycholic acid (GUDCA) reduced oxidized low-density lipoprotein uptake and inhibited foam cell formation in THP-1 macrophages.
- Oral administration of GUDCA maintained cholesterol homeostasis and attenuated atherosclerosis progression in apolipoprotein E-deficient mice.
- The changes of gut microbiota were associated with the improvement of atherosclerosis after GUDCA administration.

What Are the Clinical Implications?

- The present work provides novel insights into protective effects of GUDCA on atherosclerosis.
- GUDCA may be a potential therapeutic target in the prevention of atherosclerotic cardiovascular diseases.

Nonstandard Abbreviations and Acronyms

ApoE-/-	apolipoprotein E-deficient
GUDCA	glycoursodeoxycholic acid
LOX-1	lectin-like oxidized low-density lipoprotein receptor-1
oxLDL	oxidized low-density lipoprotein
SR-A1	scavenger receptor A1
UDCA	ursodeoxycholic acid

supplementation of live probiotics is demonstrated to ameliorate atherosclerosis in atherosclerosis-prone mice.^{10,11} Moreover, changes in gut microbiota are shown to impact the host cholesterol metabolism,⁴ intestinal permeability,¹² inflammatory reaction,¹³ and immune response,¹⁴ all of which are essential for the development of atherosclerosis. Collectively, the above evidence indicates that modulation of the gut microbiota may serve as a potent therapeutic target for atherosclerosis.

As one set of gut microbiota-derived metabolites, bile acid has been reported to be an imperative modulator of gut microbiota and functionally regulates numerous metabolic pathways in the host.^{15–17} Ursodeoxycholic acid (UDCA), a secondary bile acid derived from gut microbial 7 α / β -dehydrogenation conversion of chenodeoxycholic acid in the intestine, has been shown to exhibit multiple biological effects such as reducing circulating total cholesterol,¹⁸ suppressing foam cell formation,^{19,20} and protecting

against cardiovascular dysfunction.^{21,22} Yet its clinical utility is hampered by poor aqueous solubility.²³ Glycoursodeoxycholic acid (GUDCA), a glycine-conjugated form of UDCA, which is the main metabolite (up to 79.8%) derived from the oral administration of UDCA, is considered to be more hydrophilic and less toxic.^{24,25} Previously, GUDCA was known with neuroprotection attributable to its antiapoptosis, anti-inflammatory, and antioxidant effects.²⁶ However, its effects on metabolic disorders have been rarely explored. Interestingly, a recent study reported that GUDCA may act as an intestinal farnesoid X receptor antagonist, and substantially attenuated body weight gain and restored glucose intolerance as well as insulin resistance in a diet-induced obesity mice model, without disorders in bile acid metabolism and liver injury.²⁷ Additionally, increased serum concentration of GUDCA was associated with a decrease in hemoglobin A_{1c} as well as waist circumference in patients with type 2 diabetes mellitus.²⁸ The above evidence suggests a potential metabolic beneficial effect of GUDCA. Taken together, it is reasonable to assume that GUDCA may exhibit a protective effect on atherosclerosis. However, the potential role of GUDCA in atherosclerosis has not been investigated so far.

Hence, in line with this hypothesis, the potential role and associated mechanism of GUDCA in atherosclerosis were investigated in this study. Given the fact that foam cell formation plays a crucial role in the progression of atherosclerosis, we first explored the effect of GUDCA on oxidized low-density lipoprotein (oxLDL)-induced macrophage foam cells. Then, the impact of GUDCA on systemic metabolism and the progression of atherosclerosis were studied in an atherogenic-prone murine model. Finally, the changes of gut microbiota modulated by GUDCA and the possible association with atherosclerosis were further analyzed. To the best of our knowledge, this is the first study exploring the effects and mechanisms of GUDCA on the progression of atherosclerosis.

METHODS

The data that support the findings of this study are available from the corresponding author upon reasonable request.

Cell Culture and Experimental Conditions

Human THP-1 monocytes were obtained from National Collection of Authenticated Cell Cultures (Shanghai, China), and were cultured in RPMI-1640 medium (Gibco, Beijing, China) containing 10% fetal bovine serum (Gibco, Paisley, Scotland, UK) at 37°C in a 5% CO₂ atmosphere. Cells were used up to passage 15. THP-1 monocytes in 12-well plates were treated

with 100 nM phorbol 12-myristate 13-acetate (Sigma-Aldrich, St. Louis, MO) for 72 hours to differentiate into macrophages. Then, THP-1 macrophages were pretreated with different concentrations of GUDCA (0, 50, and 100 μ M with 0.2% dimethylsulfoxide in final concentration) for 90 minutes and subsequently co-incubated with 100 μ g/mL oxLDL (Yiyuan Biotech, Guangzhou, China) for 24 hours to induce formation of foam cells.

Oil Red O Staining

THP-1 macrophages were fixed with 4% paraformaldehyde for 30 minutes. Then, cells were rinsed twice with PBS and stained with filtered Oil red O solution (Sigma-Aldrich) at room temperature for 15 minutes, followed by destaining with 60% isopropyl alcohol for 5 seconds. Oil red O staining was observed under a light microscope, and the intensity was measured by ImageJ software (National Institutes of Health, Bethesda, MD).

Lipoprotein Uptake Assay

For the lipoprotein uptake assay, THP-1 macrophages were pretreated with different concentrations of GUDCA (0, 50, and 100 μ M) for 90 minutes, followed by coincubation with 20 μ g/mL 1,10-dioctadecyl 3,3,30,30-tetramethylindocarbocyanine-labeled oxLDL (Yiyuan Biotech, Guangzhou, China) for 24 hours in the dark at 37°C. At the end of incubation, nuclei of cells were stained with 40,6-diamidino-2-phenylindole (Thermo Fisher Scientific, Waltham, MA). Then, cells were washed with PBS and fixed with 4% paraformaldehyde for 30 minutes; 1,10-dioctadecyl 3,3,30,30-tetramethylindocarbocyanine-labeled oxLDL uptake was observed under a fluorescence microscope, and the intensity was measured by ImageJ software.

RNA Extraction and Quantitative Real-Time Reverse Transcription Polymerase Chain Reaction

Total RNA was isolated with RNAex Pro Reagent (Accurate Biology, Hunan, China), and 1 μ g of total RNA was reversely transcribed to a cDNA template using Evo M-MLVRT kit (Accurate Biology, Hunan, China). The primer sequences were deduced from PrimerBank and are listed in Table 1. Quantitative polymerase chain reaction (PCR) was performed with 1 μ L cDNA obtained above in 10 μ L containing 5 mM primers using SYBR Green Premix Pro Taq HS qPCR Kit (Accurate Biology, Hunan, China) on the LightCycler 480 system. PCR conditions were as follows: 95°C for 5 minutes, 45 cycles at 95°C for 10 seconds, and 60°C for 10 seconds. PCR results were then normalized to the expression of GAPDH in the same samples.

Animal Model

All animal experiments were performed in accordance with the *Guidelines for the Care and Use of Laboratory Animals* and were approved by the Institutional Animal Care and Use Committees of the First Affiliated Hospital of Sun Yat-sen University (Approval Number: 2019-016). Because of potential confounding effects of female sex,²⁹ 5-week-old male apolipoprotein E-deficient (ApoE^{-/-}) mice on C57BL/6J background were purchased from GemPharmatech Co. Ltd (Nanjing, China) for our in vivo experiment. All mice were housed under specific pathogen-free conditions in a control environment (20 \pm 2°C with a relative humidity of 50% to 60% and a 12-hour day/night cycle), with free access to food and water. After 1 week of acclimatization, all mice were fed a Western diet containing 45% fat (kcal/100 g) and 0.2% (wt/wt) cholesterol (TP26303, TROPHIC, Nantong, China) for 10 weeks to induce the atherosclerotic model. Then, mice were randomly divided into 2 groups: GUDCA (n=7) and control (n=5), and subsequently administered GUDCA at 50 mg/kg per day (Sigma-Aldrich; with a solution of 2% dimethylsulfoxide, 48% polyethylene glycol 400, and 50% H₂O) or its vehicle by daily oral gavage for another 18 weeks under Western diet feeding. Food intake was recorded daily, and body weight was monitored weekly. Fecal samples were collected 12 weeks after the initial intervention. At the end of the study, mice were fasted for 4 hours and blood glucose was measured from the tail tip with an ACCU-CHEK Performa glucose meter (Roche Diagnostics, Indianapolis, IN). The mice were then anesthetized with sodium pentobarbital (80 mg/kg) intraperitoneally, and blood was obtained from the retro-orbital plexus. Liver, epididymal, and retroperitoneal fat pads were collected and weighed. Liver index and adiposity index were calculated from liver weight or epididymal and retroperitoneal fat pads weights, with normalization to body weight. Tissue samples were frozen at -80°C or stored in 4% paraformaldehyde until analysis.

Lipid Profile Analysis

Levels of total cholesterol, total triglycerides, and low-density lipoprotein cholesterol in plasma and liver, as well as total cholesterol in feces were determined using commercial assay kits (Nanjing Jiancheng Bioengineering Institute, Nanjing, China). Liver and feces homogenates were obtained by an electric homogenizer. In brief, liver and fecal samples were weighed and homogenized with 9-times volume of ethyl alcohol, then centrifuged at 15 294g for 5 minutes at 4°C. The supernatants from each mouse were applied to lipid profile analysis as mentioned above.

Table 1. Polymerase Chain Reaction Primers Used for Amplification

Species	Gene	Primers
Human	<i>SR-A1</i>	5'-GCAGTGGGATCACTTTCACAA-3'
		5'-AGCTGTCATTGAGCGAGCATC-3'
	<i>CD36</i>	5'-CTTTGGCTTAATGAGACTGGGAC-3'
		5'-GCAACAAACATCACCACACCA-3'
	<i>LOX-1</i>	5'-TTGCCTGGGATTAGTAGTGACC-3'
		5'-GCTTGCTCTTGTGTAGGAGGT-3'
	<i>GAPDH</i>	5'-CTGGGCTACACTGAGCACC-3'
		5'-AAGTGGTCGTTGAGGGCAATG-3'
Mouse	<i>MCP1</i>	5'-CCACTCACCTGCTGCTACTCA-3'
		5'-TGGTGATCCTCTGTAGCTCTCC-3'
	<i>Interleukin-1β</i>	5'-TGGACCTCCAGGATGAGGACA-3'
		5'-GTTTCATCTCGGAGCCTGTAGTG-3'
	<i>TNFα</i>	5'-GGTGCCTATGTCTCAGCCTCTT-3'
		5'-GCCATAGAAGTATGAGAGGGAG-3'
	<i>SR-A1</i>	5'-CGCACGTTCAATGACAGCATCC-3'
		5'-GCAAACACAAGGAGGTAGAGAGC-3'
	<i>CD36</i>	5'-GGACATTGAGATTCTTTTCTCTG-3'
		5'-GCAAAGGCATTGGCTGGAAGAAC-3'
	<i>LOX-1</i>	5'-GTCATCCTCTGCCTGGTGTGT-3'
		5'-TGCCTTCTGCTGGGCTAACATC-3'
	<i>ABCG5</i>	5'-AGAGGGCCTCACATCAACAGA-3'
		5'-CTGACGCTGTAGGACACATGC-3'
	<i>ABCG8</i>	5'-GGTCCTTCTGATGACATCTGGC-3'
		5'-CGTCTGTCGATGCTGGTCAAGT-3'
	<i>ACAT2</i>	5'-GAGATTGTGCCAGTGTGGTGT-3'
		5'-GTGACAGTTCCTGTCCATCAG-3'
	<i>GAPDH</i>	5'-TGCACCACCAACTGCTTAG-3'
		5'-GATGCAGGGATGATGTTTC-3'

Abbreviations: ABCG5 indicates ATP-binding cassette transporter G5; ABCG8, ATP-binding cassette transporter G8; ACAT2, acyl-CoA cholesteryl acyl transferases 2; LOX-1, lectin-like oxidized low-density lipoprotein receptor-1; MCP-1, monocyte chemoattractant protein 1; SR-A1, scavenger receptor A1; and TNF α , tumor necrosis factor- α .

Biochemical Indexes Analysis

The levels of alanine aminotransferase, aspartate aminotransferase, creatinine, and lactate dehydrogenase in plasma were detected by using a Chemray-240 Automated Biochemical Analyzer (Rayto Life and Analytical Sciences, Shenzhen, China).

Histology and Immunohistochemistry Analysis

Atherosclerotic lesions were assessed as previously described.³⁰ Briefly, ice-cold PBS was perfused into vasculature through an apical left ventricular puncture; then, the aorta and heart were separated and removed immediately. To assess the plaque size at the aortic root, the samples were cut in the ascending aorta, and the proximal samples containing the aortic roots were embedded in optimal cutting temperature

compounds. Consecutive sections (7- μ m thickness) were collected from each mouse and processed for hematoxylin and eosin, Oil red O, and Masson trichrome staining according to standardized protocols. The areas of plaque, Oil red O-positive, and collagen were measured using ImageJ software. In detail, the size of the plaque was indicated as the area between the lumen border and the internal elastic lamina border in the aortic root. Immunohistochemistry was conducted using antibodies to identify macrophages (F4/80, 1:50; Servicebio, Wuhan, China) on 3 consecutive sections. Stained sections were digitally captured, and the percentage of the stained area (the stained area per total atherosclerotic lesion area) was calculated. For the analysis of the liver, the tissues were fixed in 4% paraformaldehyde, and sections were then stained for hematoxylin and eosin, Oil red O, and Sirius red. Steatosis and fibrosis were

shown as percentage of area, which were quantified by histomorphometry using ImageJ software.

Quantitative 16S rDNA Sequencing

Fecal samples were profiled for bacterial taxa using 16S rDNA gene sequencing as previously reported.³¹ Briefly, microbial DNA was extracted from feces samples using the FastDNA SPIN Kit (MP Biomedicals, Santa Ana, CA) according to the manufacturer's protocol. Amplification and sequencing of the V4 hyper-variable region of the 16S rRNA gene was performed using the validated, region-specific bacterial primers 515F and 806R. The PCR conditions consisted of an initial denaturation step of 95°C for 3 minutes; 30 cycles of 98°C for 1 minute, 98°C for 10 seconds, 50°C for 30 seconds, 72°C for 30 seconds, followed by 72°C for 5 minutes. Replicate amplicons were pooled and purified using the AxyPrep DNA purification Kit (AXYGEN, Inc, Union City, CA). Subsequently, paired-end sequencing was performed using the Miseq PE150 platform (Illumina, San Diego, CA). Operational taxonomic units were picked at 97% sequence similarity using the Greengene bacterial database for taxonomy information. Microbial composition at each taxonomic level was defined using the summarize_taxa function in Quantitative Insights Into Microbial Ecology. The abundance of each taxon was calculated by dividing the sequences pertaining to a specific taxon by the total number of bacterial sequences for that sample.

Statistical Analysis

Data are shown as the mean \pm SEM or box-and-whisker diagrams where the center line represents the median value, the boxes indicate the interquartile ranges, and the whiskers show the minimum and maximum values. Normal distribution of data was assessed with the Shapiro-Wilk test. Unpaired 2-tailed Student's *t*-test or Welch's *t*-test was used for comparing differences between control and GUDCA groups, depending on the distribution of these data. In multiple-group analysis, 1-way ANOVA was applied and followed by Dunnett's multiple comparison test. Biological replicates are indicated in figure legends. Correlations between bacterial genera and atherosclerotic lesion area are shown as linear regression, and the dashed lines indicate 95% CI of the regression line (solid line) best fit for the sample data. Correlation coefficient *r* and significance of differences were calculated by using the nonparametric Spearman correlation test. Analyses were performed using Prism 8 (GraphPad Software, La Jolla, CA) unless otherwise indicated. Compositional similarity in gut microbiota was accessed by principal components analysis based on the Bray-Curtis distance

using Unweighted UniFrac Adonis analysis.³² The results were considered statistically significant if $P < 0.05$.

RESULTS

GUDCA Inhibits Macrophage-Derived Foam Cell Formation

Considering the crucial role of macrophage-derived foam cells in the development of atherosclerosis, the in vitro studies were first carried out to verify if GUDCA plays a role in oxLDL-induced macrophage foam cell formation. By Oil red O staining, we found that GUDCA significantly decreased intracellular lipid content in THP-1 macrophages incubated with oxLDL for 24 hours (Figure 1A,C), suggesting the inhibition of macrophage-derived foam cell formation.

Since uptake of oxLDL is the initiating step of foam cell formation, we next explored whether it would be regulated by GUDCA. Interestingly, pretreating with GUDCA robustly reduced 1,10-dioctadecyl 3,3,30,30-tetramethylindocarbocyanine-labeled oxLDL (a fluorescence-labeled oxLDL) area in a dose-dependent manner (Figure 1B,D). To further determine the possible mechanism, expressions of genes mediating the uptake of oxLDL particles into macrophages including scavenger receptor A1 (SR-A1), CD36, and lectin-like oxidized low-density lipoprotein receptor-1 (LOX-1) were analyzed. Only SR-A1 mRNA level was remarkably downregulated after GUDCA treatment, while the expressions of CD36 and LOX-1 were modestly reduced without statistical significance (Figure 1E).

These data indicated that GUDCA inhibited macrophage-derived foam cell formation, a hallmark of atherosclerosis, suggesting potential improvement of GUDCA on the development of atherosclerosis.

The Effects of GUDCA on Systemic Metabolism of ApoE^{-/-} Mice

To further investigate the effects of GUDCA treatment on systemic metabolism, the male ApoE^{-/-} mice fed a Western diet were gavaged with or without GUDCA for 18 weeks (Figure 2A). GUDCA showed no influence on mouse body weight (Figure 2B) and daily food intake between the 2 groups (Figure 2C). Yet the fasting blood glucose and liver weight were significantly improved, whereas the adiposity index was unchanged (Figure 2D through 2F). By using Oil red O and Sirius red staining of liver sections, we found that GUDCA improved hepatic steatosis, while the fibrotic area was unaltered between the 2 groups (Figure 2G through 2I). Consistently, the levels of total triglycerides, total cholesterol and low-density lipoprotein cholesterol in liver were significantly reduced

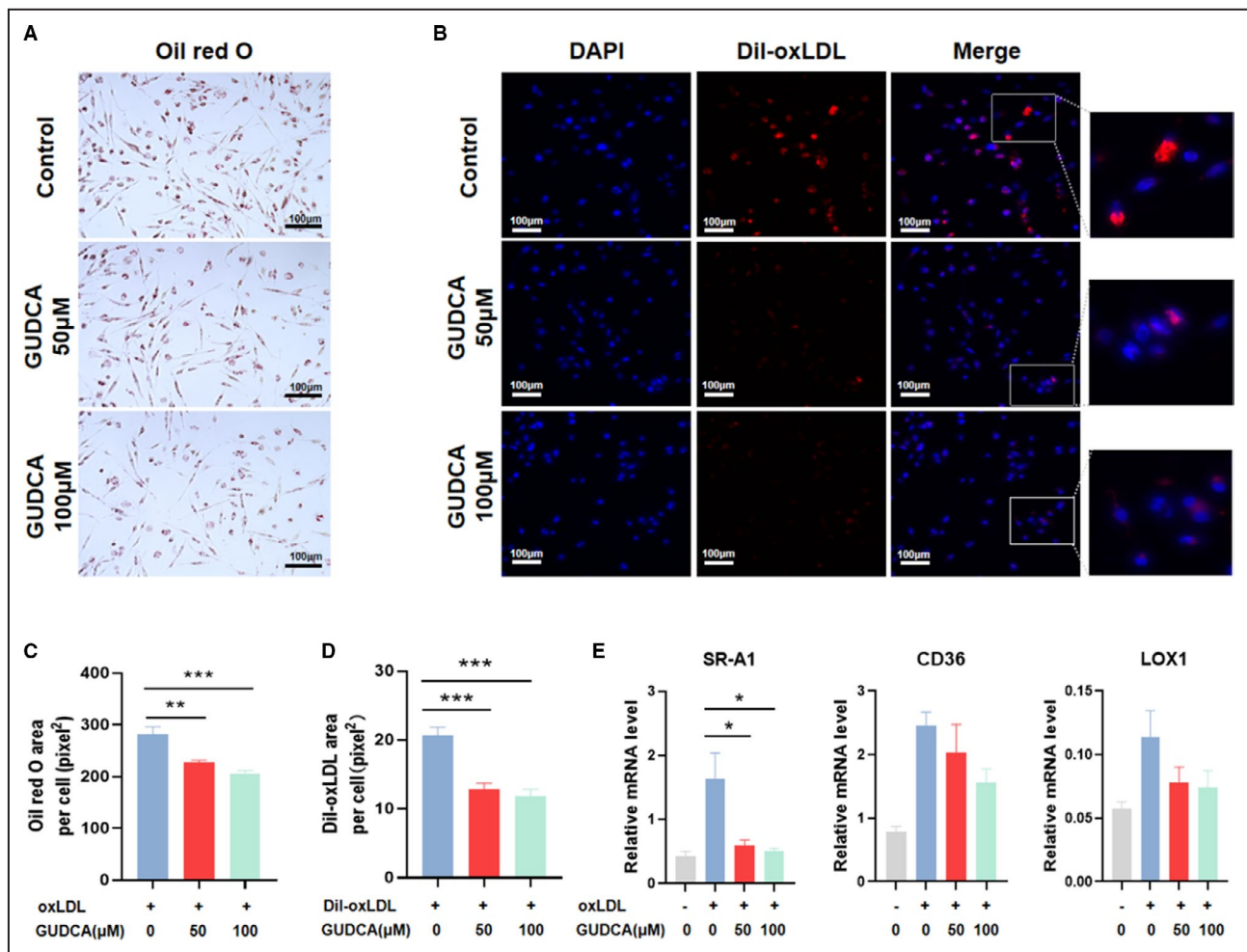


Figure 1. GUDCA inhibits macrophage-derived foam cell formation.

THP-1 macrophages were pretreated with indicated concentrations (0, 50, or 100 μ M) of GUDCA, then incubated with oxLDL or Dil-labeled oxLDL for 24 h. **A**, Representative Oil red O staining in oxLDL-induced THP-1 macrophages. **B**, Fluorescent images of THP-1 macrophages incubated with Dil-labeled oxLDL. Scale bar, 100 μ m. **C**, Quantitative analyses of Oil red O and **(D)** Dil-oxLDL positive area (representative as pixel² per cell). **E**, Relative mRNA expression of genes involved in oxLDL uptake; GAPDH mRNA was used as internal control. Data are representative of three independent experiments and shown as mean \pm SEM. Statistical analyses were performed with 1-way ANOVA and followed by Dunnett multiple comparisons. * P <0.05, ** P <0.01 and *** P <0.001 vs control. Dil-oxLDL indicates 1,10-dioctadecyl-3,3',3'',3'''-tetramethylindocarbocyanine-labeled oxidized low-density lipoprotein; GUDCA, glycoursoxycholeic acid; LOX-1, lectin-like oxidized low-density lipoprotein receptor-1; oxLDL, oxidized low-density lipoprotein; and SR-A1, scavenger receptor A1.

with GUDCA treatment, suggesting that GUDCA improved lipid metabolism and subsequently prevented hepatic steatosis development. In addition, total cholesterol and low-density lipoprotein cholesterol in plasma were significantly lower in GUDCA mice, while total triglycerides showed no difference (Figure 2J,K). Given that fecal output represents one of the most important pathways on maintenance of cholesterol homeostasis, we further investigated fecal cholesterol excretion in mice. As a result, we found that the level of fecal cholesterol in mice administered GUDCA was robustly increased (Figure 2L), suggesting that GUDCA promoted fecal cholesterol excretion. Moreover, quantitative PCR analysis showed

that GUDCA significantly upregulated expressions of ATP-binding cassette transporter G5 and G8, and downregulated expression of acyl-CoA cholesterol acyl transferases 2 in the ileum of mice (Figure S1). Taken together, these data indicated that GUDCA exerted a metabolic beneficial effect, especially with the cholesterol homeostasis, on Western diet-induced metabolic disorders of ApoE^{-/-} mice.

Furthermore, the levels of alanine aminotransferase and aspartate aminotransferase in plasma were lower in mice administered with GUDCA, while creatinine as well as lactate dehydrogenase were unchanged, suggesting that the current dose of GUDCA was safe, with no obvious organ toxicity in mice (Figure S2).

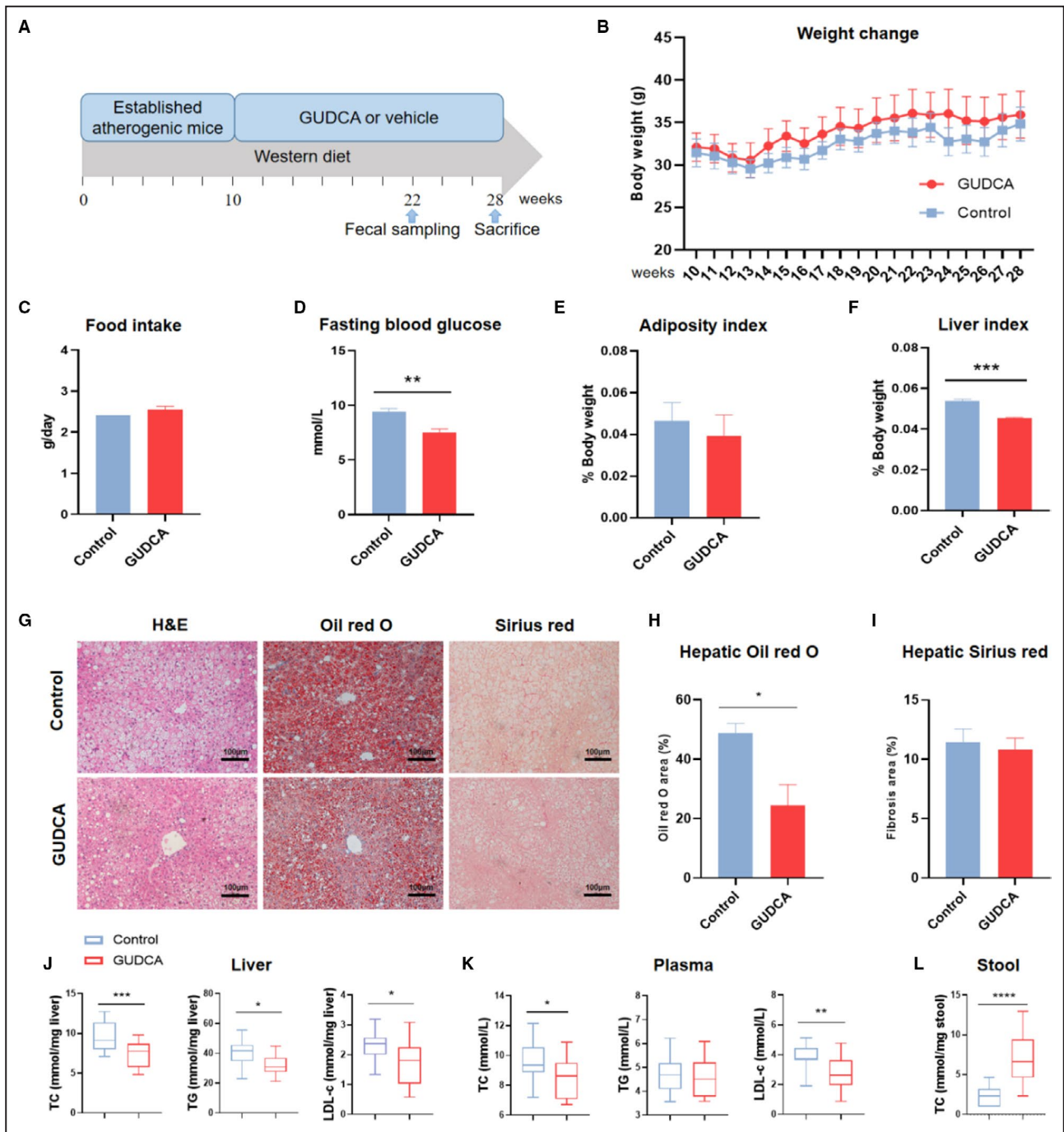


Figure 2. The effects of GUDCA in systemic metabolism of ApoE^{-/-} mice under Western diet.

After a 10 weeks of Western diet feeding, ApoE^{-/-} mice were randomly divided into 2 groups and subsequently treated with GUDCA or its vehicle for 18 weeks. **A**, The animal experimental design; **B**, body weight changes; and **C**, average daily food intake after intervention. n=5 for control, n=7 for GUDCA. **D**, Blood glucose was measured after 4 h of fasting at the day of euthanasia. n=4 for control, n=6 for GUDCA. **E**, Liver index; and **F**, adiposity index were normalized to body weight. n=4 mice per groups. **G**, Liver histology by H&E (left), Oil red O (middle), and Sirius red (right) staining. Scale bar, 100 μm. **H**, Quantitative analysis of Oil red O area; and **I**, fibrosis area (shown as percentage of area). n=4 mice per groups, with 10 randomized high-power fields per mouse. Data are presented with mean±SEM. **J**, Liver; **K**, plasma; and **L**, stool lipid profile. n=5 for Control, n=7 for GUDCA, with three duplicates for each test. Data are represented as box plots, where the boxes indicate the median and the interquartile ranges and the whiskers show as the minimum and maximum values. Statistical analyses were performed with unpaired 2-tailed Student’s *t*-test with or without Welch correction, depending on the distribution of these data. **P*<0.05, ***P*<0.01 and ****P*<0.001 vs control. ApoE^{-/-} indicates apolipoprotein E-deficient; GUDCA, glyoursodeoxycholic acid; H&E, hematoxylin and eosin; LDL-c, low-density lipoprotein cholesterol TC, total cholesterol; and TG, total triglycerides.

GUDCA Administration Attenuates Atherosclerosis in ApoE^{-/-} Mice

To ascertain whether GUDCA protects against atherosclerosis in vivo, the plaque lesions of the aortic root were assessed. GUDCA administration resulted

in a 39% reduction of plaque area in ApoE^{-/-} mice (Figure 3C,G). Lipid deposition detected with Oil red O sections showed that GUDCA also decreased intravascular lipid area (Figure 3D,H). In addition, a higher level of collagen, which was defined by Masson trichrome staining, indicated that GUDCA

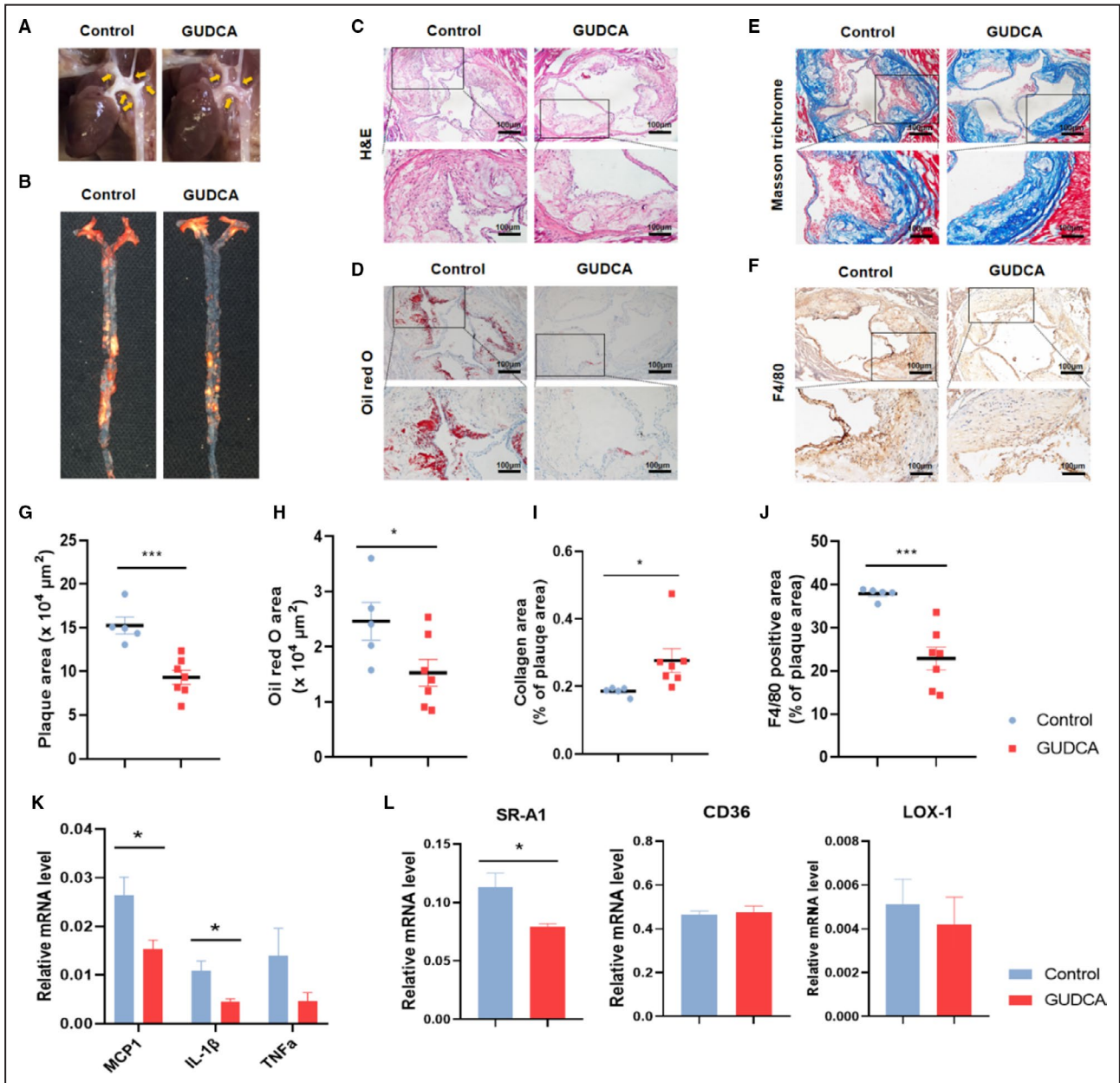


Figure 3. GUDCA administration protects against atherosclerosis in ApoE^{-/-} mice.

A, Representative in situ; and **B**, Oil red O staining en-face images of aorta. **C**, Representative photographs of H&E; **D** Oil red O; and **E**, Masson trichrome staining; and **F**, immunohistochemistry staining of F4/80-positive macrophages in aortic root. The boxed areas are enlarged below. Scale bar, 100 μm. **G**, Quantitative analyses of plaque area; **H**, Oil red O area; **I**, collagen area; and **J**, F4/80-positive area (shown as percentage of plaque area) in aortic root. n=5 for control, n=7 for GUDCA, with 3 consecutive sections per mouse. The symbols indicate values for each mouse, with lines represent mean±SEM. **K**, Relative mRNA levels of genes involved in inflammation; and **L**, oxLDL uptake; GAPDH mRNA was used as internal control. n=3–4 mice per groups. Data are representative of 2 independent experiments and shown as mean±SEM. Significance was calculated by unpaired 2-tailed Student’s t-test with or without Welch correction, depending on the distribution of these data. *P<0.05, **P<0.01, and ***P<0.001 vs control. ApoE^{-/-} indicates apolipoprotein E-deficient; GUDCA, glyoursodeoxycholic acid; H&E, hematoxylin and eosin; LOX-1, lectin-like oxidized low-density lipoprotein receptor-1; MCP1, monocyte chemoattractant protein 1; SR-A1, scavenger receptor A1; and TNFα, tumor necrosis factor-α.

promoted the stability of the atherosclerotic plaque (Figure 3E,I). Furthermore, the amount of macrophages was significantly reduced (Figure 3F,J), and the mRNA levels of monocyte chemoattractant protein 1 and interleukin-1 β were downregulated in the aorta of GUDCA mice (Figure 3K), suggesting that GUDCA ameliorated the local chronic inflammation in mice aortas. Finally, consistent with the data in vitro, the mRNA level of SR-A1 in the aorta was downregulated in the presence of GUDCA (Figure 3L). Taken together, these findings suggested that supplementation of GUDCA attenuated atherosclerosis progression in ApoE^{-/-} mice.

GUDCA Administration Alters the Composition of Gut Microbiota in ApoE^{-/-} Mice

As previously reported, gut microbiota is associated with the progression of atherosclerosis.³³ Although bile acid represents a potent regulator of gut microbiota, the influence of GUDCA on gut microbiota under atherosclerotic condition remains unknown. Thus, we analyzed the fecal microbiota in ApoE^{-/-} mice with or without GUDCA supplementation by 16S rDNA gene sequencing. Compared with control mice, the number of operational taxonomic units, microbial diversity (as shown by the Shannon index) and evenness (as shown by chao1 estimator) were not changed after GUDCA intervention (Figure 4A through 4C). However, principal components analysis showed that the cluster of gut microbiota were separated because of GUDCA intervention, which was further confirmed by an unweighted adonis test (Figure 4D). At the phylum level, the fecal microbiota of all mice was dominated by *Firmicutes* (38.1%), which were followed by *Bacteroidetes* (34.7%), whereas the relative abundance of *Firmicutes* phyla in GUDCA mice was lower than that in control mice (Figure 4E). Since a higher ratio of *Firmicutes*/*Bacteroidetes* has been linked to metabolic disorders,³⁴ oral supplementation of GUDCA showed a modestly, albeit not significantly ($P=0.2971$), decreased *Firmicutes*/*Bacteroidetes* ratio in mice fed a Western diet (Figure 4F), suggesting a potential beneficial effect of GUDCA on the gut microbiota composition. Notably, *Alloprevotella* together with *Parabacteroides* genera, which belong to the *Bacteroidetes* phylum and are metabolically beneficial,³⁵ were significantly increased with GUDCA supplementation. On the contrary, the potentially harmful bacterial genera, such as *Turicibacter* and *Alistipes*, were remarkably depleted (Figure 4H). Altogether, these data showed that GUDCA represented a potent beneficial regulator to Western diet-induced gut microbiota dysbiosis.

GUDCA-Altered Gut Microbiota Correlates With Atherosclerosis

To further investigate the association of the GUDCA-altered gut microbiota and the progression of atherosclerosis, multiple correlation analyses were performed. Interestingly, GUDCA-enriched *Parabacteroides* and *Alloprevotella* were significantly negatively correlated with the plaque area in the aortic root (Figure 5A,B), as a positive correlation was observed in the GUDCA-depleted genera *Turicibacter* and *Alistipes* (Figure 5C,D). These findings indicated that the changes of microbiota taxa associated with GUDCA intervention was potentially correlated with the improvement of atherosclerosis.

DISCUSSION

The regulatory effect of GUDCA in the progression of atherosclerosis has not yet been studied, though a few reports suggested that GUDCA may improve metabolic dysfunction in mice with diet-induced obesity.²⁷ In the present study, we found that GUDCA inhibited foam cell formation, maintained cholesterol homeostasis, and attenuated atherosclerosis progression. Moreover, the changes of gut microbiota modulated by GUDCA were correlated with the improvement of atherosclerosis. Taken together, our results for the first time demonstrated that GUDCA improved atherosclerosis and may serve as a potential therapeutic molecule in the clinical treatment of atherosclerosis.

The formation of foam cells is a well-established hallmark of atherosclerosis.³⁶ Excessive influx of oxLDL leads to the accumulation of esterified cholesterol in macrophages and thereby aggravates the conversion of foam cells. Thereafter, increased foam cells subsequently induce intravascular lipid deposition, facilitate local chronic inflammation, and thus accelerate atherosclerosis progression.³⁶ In this process, the expressions of macrophage scavenger receptor family members (such as SR-A1, CD36, and LOX-1) are essential because of their unique property of mediating uptake of oxLDL. Knockdown of SR-A1 or CD36 has been shown to efficaciously reduce the generation of foam cells and protect against the progression of atherosclerosis, which indicates that these receptors may act as potential therapeutic targets for atherosclerosis.^{37,38} In the current study, we found that GUDCA treatment significantly reduced oxLDL uptake as well as neutral lipid deposition in human macrophages. In addition, the expression of SR-A1 was repressed in the presence of GUDCA in vitro and in vivo, suggesting an inhibitory effect of GUDCA on SR-A1. Despite the fact that detailed mechanisms are not fully understood, extracellular-signal-regulated kinase signaling is presumably responsible for the SR-A1-mediated

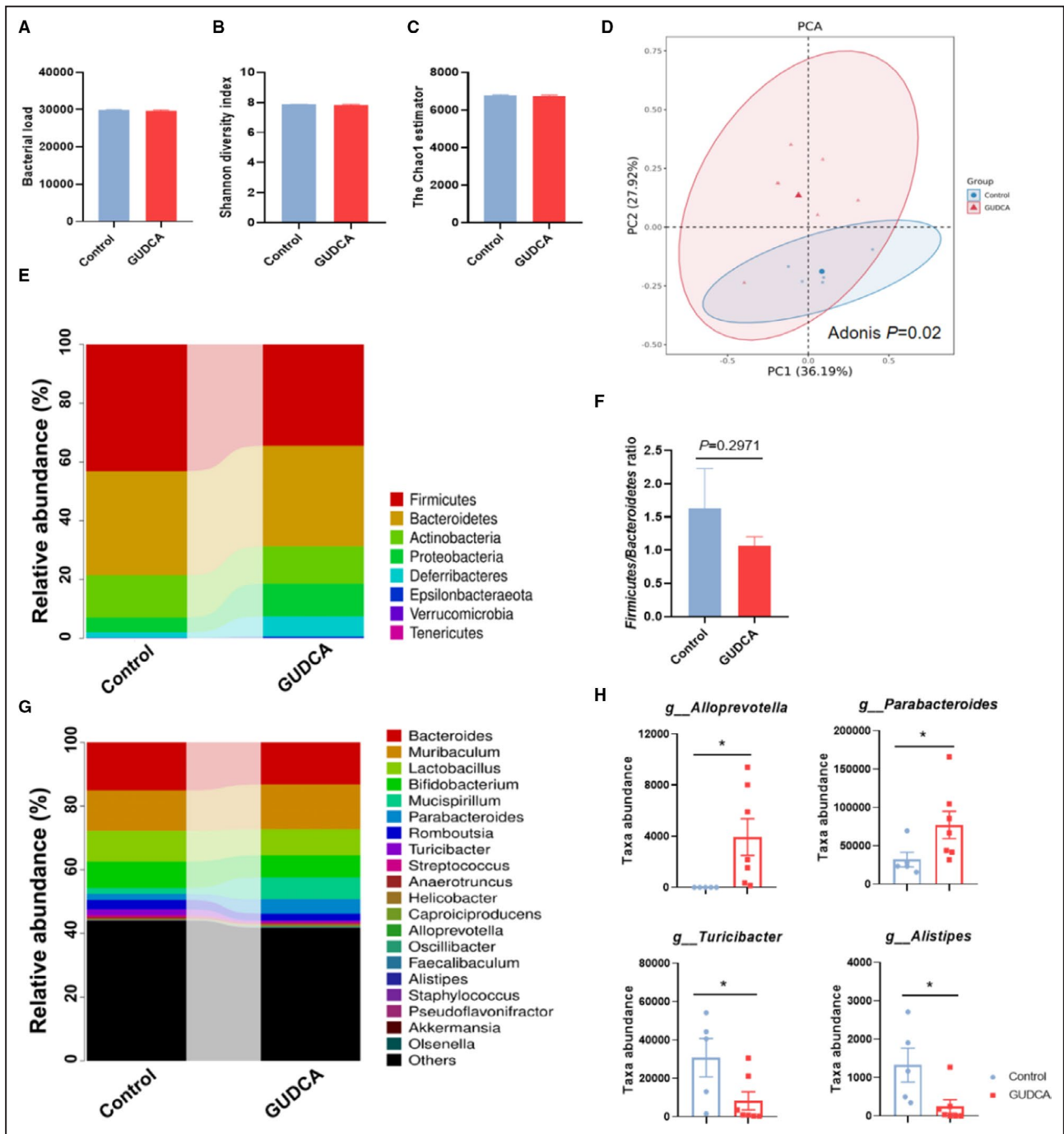


Figure 4. GUDCA administration alters the composition of gut microbiota in ApoE^{-/-} mice.

Feces of each mouse were collected after 12 weeks of treatment with or without GUDCA, and analyzed by utilization of 16S rDNA sequencing on V4 region. **A**, Operational taxonomic unit abundance in the feces between control and GUDCA. **B**, Shannon diversity index; and **C**, the Chao1 estimator in α -diversity analysis. Data are shown as mean \pm SEM. **D**, Principal component analysis (PCA) from each group. The dissimilarity was calculated by using unweighted adonis test. **E**, Microbiota compositions at the phylum level. **F**, Representative of the *Firmicutes/Bacteroidetes* ratio between groups. Data are shown as mean \pm SEM. **G**, Microbiota compositions at the genus level. **H**, Disparate microbial genus between control and GUDCA mice were assessed by Metastats analysis. The symbols indicate values for each mouse, with bars represent mean \pm SEM. n=5 in Control group, n=7 in GUDCA group. * P <0.05, ** P <0.01, and *** P <0.001 vs control. ApoE^{-/-} indicates apolipoprotein E-deficient; and GUDCA, glyoursodeoxycholic acid.

lipids internalization.³⁹ While the impact of GUDCA on extracellular-signal-regulated kinase pathway is still unknown, indirect evidence from UDCA, the

nonconjugated precursor of GUDCA, is shown to suppress the phosphorylation of extracellular-signal-regulated kinase in macrophages.⁴⁰ Further study is

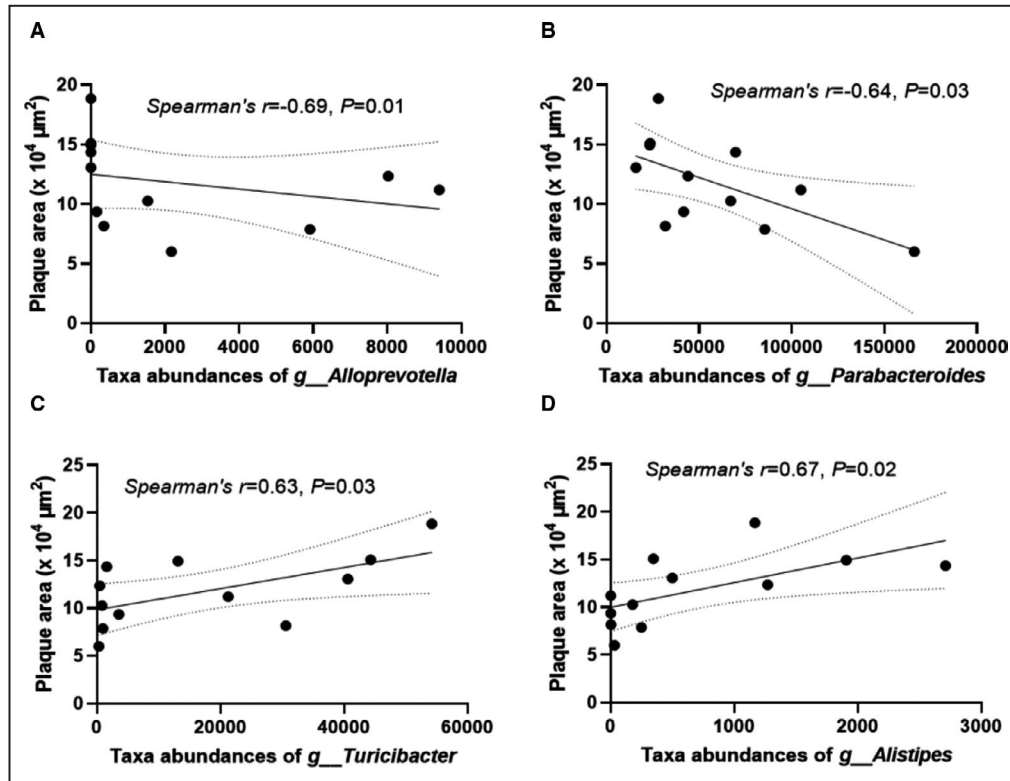


Figure 5. GUDCA-associated gut microbiota correlated with atherosclerotic plaque area. A, Spearman correlations between the taxa abundances of *Alloprevotella*; B, *Parabacteroides*; C, *Turicibacter*; and D, *Alistipes* and plaque lesion area in the aortic root. n=5 in control group, n=7 in GUDCA group.

needed to clarify the molecular mechanisms involved in the inhibitory effect on SR-A1 of GUDCA. Moreover, we found in mice aortas that GUDCA decreased macrophage infiltration and downregulated mRNA levels of monocyte chemoattractant protein 1 and inflammatory cytokines such as interleukin-1 β , suggesting that it exerted an effect of anti-inflammation. Taken all together, although the exact mechanism was not completely clarified, our study preliminarily demonstrated that GUDCA inhibited foam cell formation, ameliorated chronic inflammation, and protected against the progression of atherosclerosis.

Although the use of hydroxy-methylglutaryl-coenzyme A reductase inhibitors or statins efficaciously reduces the incidence of ASCVD, thousands of patients avoid these lifesaving medications because of the presence of or concern about statin-associated adverse effects.^{41,42} Nowadays, ASCVD remains the leading cause of death globally. Accordingly, developing novel drugs targeting the regulation of cholesterol metabolism is imperative. In recent years, proprotein convertase subtilisin/kexin 9 inhibitors, a novel cholesterol-lowering drug, were shown to strongly reduce cholesterol levels and have an incremental favorable effect on clinical outcomes in patients with atherosclerotic disease.⁴³ However, numerous side

effects such as injection-site reactions, influenza-like illness and myalgia have been noticed.⁴⁴ In addition, a recent study reported that deficiency in proprotein convertase subtilisin/kexin 9 might exacerbate hepatic steatosis and induce liver injury attributable to increased uptake and accumulation of fatty acids in the liver.⁴⁵ As an endogenous natural compound, bile acid has been long known as a regulator of cholesterol homeostasis.⁴⁶ UDCA, which was approved by the US Food and Drug Administration and largely used in the treatment of hepatobiliary diseases, is associated with a favorable cholesterol-lowering effect.^{47,48} However, a series of “unanticipated” toxicities were noted, which might be partially attributed to the potency that UDCA might biologically convert into lithocholic acid and induced DNA strand breakage.⁴⁹ As a conjugated form of UDCA, the biological effects of GUDCA may be partially overlapped with UDCA. Excitingly, the metabolic beneficial effect of GUDCA was unveiled lately,^{27,28} though whether GUDCA may impact on cholesterol homeostasis remains unknown. Herein, our data showed that oral administration of GUDCA significantly promoted transintestinal cholesterol excretion and attenuated circulating and hepatic cholesterol, suggesting a beneficial cholesterol-lowering effect of GUDCA. Additionally, GUDCA was shown to improve

insulin resistance and ameliorate liver steatosis, both of which were supposed to be the risk factors for atherosclerosis. Furthermore, our data showed that the levels of plasma alanine aminotransferase and aspartate aminotransferase were lower after GUDCA administration, which was in line with the previous study,²⁷ while creatinine and lactate dehydrogenase were unchanged. These results indicated no obvious organ toxicity, at least in liver and renal functions, after GUDCA administration. As mentioned above, GUDCA might be an alternative candidate for the management of disrupted cholesterol homeostasis as well as ASCVD. Because of a lack of evidence in clinical application, the safety and effectiveness of GUDCA still need to be further determined in the future.

Modulation of gut microbiota is considered a potential therapeutic target of atherosclerosis.^{50,51} Numerous studies on gut microbiota has revealed that the alteration of the *Firmicutes/Bacteroidetes* ratio is linked to metabolic disorders.³⁴ Additionally, the ratio of *Firmicutes/Bacteroidetes* is significantly elevated in ApoE^{-/-} mice fed a Western diet⁵² as well as patients with ASCVD.⁵³ In this study, we found that oral administration of GUDCA modestly normalized the *Firmicutes/Bacteroidetes* ratio, which implied that GUDCA exhibited a beneficial effect on the Western diet-associated gut microbiota dysbiosis. Recently, as reported by Van den Bossche and colleagues,⁵⁴ short-term oral administration of GUDCA in a dose of 500 mg/kg/day increased the abundance of *Akkermansia muciniphila* in a dextran sodium sulfate-induced colitis mouse model. However, no change of the taxa abundance of *Akkermansia muciniphila* was observed (data not shown), at least in our study; this conflict may be attributed to the differences in dose and pathological state. Intriguingly, we found that GUDCA administration significantly increased the abundances of *Alloprevotella* and *Parabacteroides*, which were negatively correlated with plaque size in mice aortas. As reported previously, both were considered as metabolic protective bacteria, which were mainly found in the gut of healthy individuals⁵⁵ and mostly depleted in patients with metabolic disorders such as ASCVD.^{56,57} In consonance with our findings, increased *Parabacteroides* along with the improvement of atherosclerosis was observed in ApoE^{-/-} mice treated with lingonberries.⁵⁸ Similarly, in rats with diet-induced hypercholesterolemia, treatment with atorvastatin strikingly reduced the cholesterol level and increased the relative abundance of *Parabacteroides*.⁵⁹ In addition, enrichment of *Alloprevotella* was associated with lower lifetime CVD risk among Bogalusa Heart Study participants.⁵⁶ The above evidence strongly implies that *Alloprevotella* and *Parabacteroides* might somehow exhibit a beneficial effect on the improvement of atherosclerosis associated with GUDCA. Conversely, we also found

that *Turicibacter* and *Alistipes* were depleted after GUDCA treatment, along with a positive correlation to plaque size. In line with our observation, an increase of *Turicibacter* has been associated with imbalanced lipid metabolism,⁶⁰ hypertension,⁶¹ and higher levels of trimethylamine N-oxide.⁶² Other than *Turicibacter*, evidence for the involvement of *Alistipes* in CVD is contradictory.⁶³ Further studies are needed to illustrate the association between *Alistipes* and CVD. Taken together, our data suggested a probable association between the amelioration of atherosclerosis and the changes of gut microbiota after GUDCA administration.

There are several limitations in our study. First, although a potential linkage was indicated in our study, it is still unknown whether the improved microbial conditions mediate the effect of GUDCA on the prevention of atherosclerosis. Future studies of fecal microbiota transplantation in germ-free mice should be conducted to clarify the causal role of gut microbiota in GUDCA-associated protection of atherosclerosis. Second, given that cholesterol levels might impact the microbial conditions,⁶⁴ it is still hard to draw a conclusion whether the better microbial conditions were directly caused by GUDCA or induced by the reduced cholesterol level. Studies should be conducted to further investigate the direct interactions between GUDCA and gut microbiota. Third, even though there are numerous advantages of using a mouse model in gut microbiota studies to explore more insights into the pathological mechanisms of human diseases, it still has a long way to go in translating such results from a murine model to humans because of the differences between the 2 systems.^{65,66} For example, the composition of gut microbiota and relative abundance of most of the dominant genera are quite disparate in mice and humans.⁶⁷ Therefore, the influences of GUDCA on gut microbiota in human beings require further elucidation.

In summary, although there are several limitations in this study, we for the first time, to our knowledge, report that oral administration of GUDCA attenuates Western diet-induced atherosclerosis in ApoE^{-/-} mice, possibly via inhibiting foam cell formation, improving cholesterol homeostasis, and remodeling gut microbiota. Although complete understanding of the impact of GUDCA on atherosclerosis still requires further investigation, the present study provides novel insights into protective effects of GUDCA on atherosclerosis, suggesting GUDCA as a potential therapeutic target in prevention/treatment of atherosclerotic cardiovascular diseases.

ARTICLE INFORMATION

Received October 21, 2020; accepted February 22, 2021.

Affiliations

From the Division of Vascular Surgery (K.H., C.L., M.P., Z.L., G.C.), National-Guangdong Joint Engineering Laboratory for Diagnosis and Treatment of

Vascular Diseases (K.H., C.L., M.P., R.L., Z.L., G.C.) and Animal Center (Q.S.), First Affiliated Hospital, Sun Yat-sen University, Guangzhou, China; Zhongshan School of Medicine, Sun Yat-sen University, Guangzhou, China (Z.G.); and Guangdong Provincial Key Laboratory of Malignant Tumor Epigenetics and Gene Regulation, Medical Research Center, Sun Yat-Sen Memorial Hospital, Guangzhou, China (S.C.).

Sources of Funding

This work was supported by the the National Natural Science Foundation of China (grant numbers 81970416; 81670439; 81970406), The National Science Foundation of Young Scientists of China (grant number 81900757), and the Fundamental Research Funds for the Central Universities (grant number 20ykzd11).

Disclosures

None.

Supplementary Material

Figures S1-S2

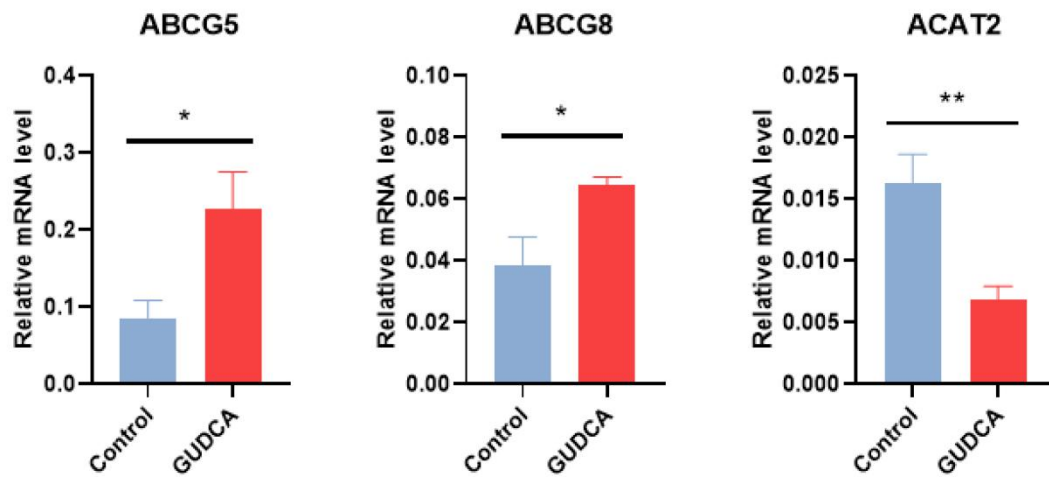
REFERENCES

- Piepoli MF, Hoes AW, Agewall S, Albus C, Brotons C, Catapano AL, Cooney M-T, Corrà U, Cosyns B, Deaton C, et al. 2016 European guidelines on cardiovascular disease prevention in clinical practice: the sixth joint task force of the European society of cardiology and other societies on cardiovascular disease prevention in clinical practice (constituted by representatives of 10 societies and by invited experts) developed with the special contribution of the European Association for Cardiovascular Prevention & Rehabilitation (EACPR). *Eur Heart J*. 2016;37:2315–2381. DOI: 10.1093/eurheartj/ehw106.
- Nasu K, Terashima M, Habara M, Ko E, Ito T, Yokota D, Ishizuka S, Kurita T, Kimura M, Kinoshita Y, et al. Impact of cholesterol metabolism on coronary plaque vulnerability of target vessels: a combined analysis of virtual histology intravascular ultrasound and optical coherence tomography. *JACC Cardiovasc Interv*. 2013;6:746–755. DOI: 10.1016/j.jcin.2013.02.018
- Gidding SS, Allen NB. Cholesterol and atherosclerotic cardiovascular disease: a lifelong problem. *J Am Heart Assoc*. 2019;8:e012924. DOI: 10.1161/JAHA.119.012924.
- Le Roy T, Lécuyer E, Chassaing B, Rhimi M, Lhomme M, Boudebbouze S, Ichou F, Haro Barceló J, Huby T, Guerin M, et al. The intestinal microbiota regulates host cholesterol homeostasis. *BMC Biol*. 2019;17:94. DOI: 10.1186/s12915-019-0715-8.
- Herrington W, Lacey B, Sherliker P, Armitage J, Lewington S. Epidemiology of atherosclerosis and the potential to reduce the global burden of atherothrombotic disease. *Circ Res*. 2016;118:535–546. DOI: 10.1161/CIRCRESAHA.115.307611.
- Wong ND, Zhao Y, Quek RGW, Blumenthal RS, Budoff MJ, Cushman M, Garg P, Sandfort V, Tsai M, Lopez JAG. Residual atherosclerotic cardiovascular disease risk in statin-treated adults: the multi-ethnic study of atherosclerosis. *J Clin Lipidol*. 2017;11:1223–1233. DOI: 10.1016/j.jacl.2017.06.015.
- Claesson MJ, Jeffery IB, Conde S, Power SE, O'Connor EM, Cusack S, Harris HMB, Coakley M, Lakshminarayanan B, O'Sullivan O, et al. Gut microbiota composition correlates with diet and health in the elderly. *Nature*. 2012;488:178–184. DOI: 10.1038/nature11319.
- Du M, Yu JS, Yang YZ, Yan F, Chen ZY. Microbes in oncology: controllable strategies for bacteria therapy. *BIO Integration*. 2020;1:185–192. DOI: 10.15212/bioi-2020-0025.
- Jie Z, Xia H, Zhong S-L, Feng Q, Li S, Liang S, Zhong H, Liu Z, Gao Y, Zhao H, et al. The gut microbiome in atherosclerotic cardiovascular disease. *Nat Commun*. 2017;8:845. DOI: 10.1038/s41467-017-00900-1.
- Li J, Lin S, Vanhoutte PM, Woo CW, Xu A. Akkermansia muciniphila protects against atherosclerosis by preventing metabolic endotoxemia-induced inflammation in ApoE^{-/-} mice. *Circulation*. 2016;133:2434–2446. DOI: 10.1161/CIRCULATIONAHA.115.019645.
- Yoshida N, Emoto T, Yamashita T, Watanabe H, Hayashi T, Tabata T, Hoshi N, Hatano N, Ozawa G, Sasaki N, et al. Bacteroides vulgatus and Bacteroides dorei reduce gut microbial lipopolysaccharide production and inhibit atherosclerosis. *Circulation*. 2018;138:2486–2498. DOI: 10.1161/CIRCULATIONAHA.118.033714.
- Mouries J, Brescia P, Silvestri A, Spadoni I, Sorribas M, Wiest R, Mileti E, Galbati M, Invernizzi P, Adorini L, et al. Microbiota-driven gut vascular barrier disruption is a prerequisite for non-alcoholic steatohepatitis development. *J Hepatol*. 2019;71:1216–1228. DOI: 10.1016/j.jhep.2019.08.005.
- Xu C, Lee SK, Zhang D, Frenette PS. The gut microbiome regulates psychological-stress-induced inflammation. *Immunity*. 2020;53:417–428. DOI: 10.1016/j.immuni.2020.06.025.
- Kim M, Galan C, Hill AA, Wu WJ, Fehlner-Peach H, Song HW, Schady D, Bettini ML, Simpson KW, Longman RS, et al. Critical role for the microbiota in CX3CR1(+) intestinal mononuclear phagocyte regulation of intestinal T cell responses. *Immunity*. 2018;49:151–163. DOI: 10.1016/j.immuni.2018.05.009.
- Just S, Mondot S, Ecker J, Wegner K, Rath E, Gau L, Streidl T, Hery-Arnaud G, Schmidt S, Lesker TR, et al. The gut microbiota drives the impact of bile acids and fat source in diet on mouse metabolism. *Microbiome*. 2018;6:134. DOI: 10.1186/s40168-018-0510-8.
- Staley C, Weingarden AR, Khoruts A, Sadowsky MJ. Interaction of gut microbiota with bile acid metabolism and its influence on disease states. *Appl Microbiol Biotechnol*. 2017;101:47–64. DOI: 10.1007/s00253-016-8006-6.
- Wei M, Huang F, Zhao L, Zhang Y, Yang W, Wang S, Li M, Han X, Ge K, Qu C, et al. A dysregulated bile acid-gut microbiota axis contributes to obesity susceptibility. *EBioMed*. 2020;55:102766. DOI: 10.1016/j.ebiom.2020.102766.
- Cicognani C, Malavolti M, Morselli-Labate AM, Talarico R, Zamboni L, Sama C. Effect of ursodeoxycholic acid administration in patients with primary hypercholesterolaemia. *Clin Drug Invest*. 1999;18:263–269. DOI: 10.2165/00044011-199918040-00002.
- Chung J, An SH, Kang SW, Kwon K. Ursodeoxycholic acid (UDCA) exerts anti-atherogenic effects by inhibiting RAGE signaling in diabetic atherosclerosis. *PLoS One*. 2016;11:e0147839. DOI: 10.1371/journal.pone.0147839.
- Bode N, Grebe A, Kerksiek A, Lutjohann D, Werner N, Nickenig G, Latz E, Zimmer S. Ursodeoxycholic acid impairs atherogenesis and promotes plaque regression by cholesterol crystal dissolution in mice. *Biochem Biophys Res Commun*. 2016;478:356–362. DOI: 10.1016/j.bbrc.2016.07.047.
- von Haehling S, Schefold JC, Jankowska EA, Springer J, Vazir A, Kalra PR, Sandek A, Fauler G, Stojakovic T, Trauner M, et al. Ursodeoxycholic acid in patients with chronic heart failure: a double-blind, randomized, placebo-controlled, crossover trial. *J Am Coll Cardiol*. 2012;59:585–592. DOI: 10.1016/j.jacc.2011.10.880.
- Sinisalo J, Vanhanen H, Pajunen P, Vapaatalo H, Nieminen MS. Ursodeoxycholic acid and endothelial-dependent, nitric oxide-independent vasodilatation of forearm resistance arteries in patients with coronary heart disease. *Br J Clin Pharmacol*. 1999;47:661–665. DOI: 10.1046/j.1365-2125.1999.00940.x.
- Dosa PI, Ward T, Castro RE, Rodrigues CM, Steer CJ. Synthesis and evaluation of water-soluble prodrugs of ursodeoxycholic acid (UDCA), an anti-apoptotic bile acid. *ChemMedChem*. 2013;8:1002–1011. DOI: 10.1002/cmdc.201300059.
- Rudolph G, Kloeters-Plachky P, Sauer P, Stiehl A. Intestinal absorption and biliary secretion of ursodeoxycholic acid and its taurine conjugate. *Eur J Clin Invest*. 2002;32:575–580. DOI: 10.1046/j.1365-2362.2002.01030.x.
- Ferreira M, Coxito PM, Sardao VA, Palmeira CM, Oliveira PJ. Bile acids are toxic for isolated cardiac mitochondria: a possible cause for hepatic-derived cardiomyopathies? *Cardiovasc Toxicol*. 2005;5:63–73. DOI: 10.1385/CT:5:1:063.
- Grant SM, DeMorrow S. Bile acid signaling in neurodegenerative and neurological disorders. *Int J Mol Sci*. 2020;21:5982. DOI: 10.3390/ijms21175982.
- Sun L, Xie C, Wang G, Wu Y, Wu Q, Wang X, Liu J, Deng Y, Xia J, Chen BO, et al. Gut microbiota and intestinal FXR mediate the clinical benefits of metformin. *Nat Med*. 2018;24:1919–1929. DOI: 10.1038/s41591-018-0222-4.
- Li W, Liu R, Li X, Tao B, Zhai N, Wang X, Li Q, Zhang Y, Gu W, Wang W, et al. Saxagliptin alters bile acid profiles and yields metabolic benefits in drug-naïve overweight or obese type 2 diabetes patient. *J Diabetes*. 2019;11:982–992. DOI: 10.1111/1753-0407.12956.
- Zhang G, Li C, Zhu N, Chen Y, Yu Q, Liu E, Wang R. Sex differences in the formation of atherosclerosis lesion in ApoE^{-/-} mice and the effect of 17 β -estradiol on protein S-nitrosylation. *Biomed Pharmacother*. 2018;99:1014–1021. DOI: 10.1016/j.biopha.2018.01.145.

30. Mohanta S, Yin C, Weber C, Hu D, Habenicht AJ. Aorta atherosclerosis lesion analysis in hyperlipidemic mice. *Bio Protoc.* 2016;6:e1833. DOI: 10.21769/BioProtoc.1833.
31. Vandeputte D, Kathagen G, D'hoel K, Vieira-Silva S, Valles-Colomer M, Sabino J, Wang J, Tito RY, De Commer L, Darzi Y, et al. Quantitative microbiome profiling links gut community variation to microbial load. *Nature.* 2017;551:507–511. DOI: 10.1038/nature24460.
32. Liu F, Fan C, Zhang L, Li Y, Hou H, Ma Y, Fan J, Tan Y, Wu T, Jia S, et al. Alterations of gut microbiome in Tibetan patients with coronary heart disease. *Front Cell Infect Microbiol.* 2020;10:373. DOI: 10.3389/fcimb.2020.00373.
33. Jonsson AL, Backhed F. Role of gut microbiota in atherosclerosis. *Nat Rev Cardiol.* 2017;14:79–87. DOI: 10.1038/nrcardio.2016.183.
34. Ley RE, Turnbaugh PJ, Klein S, Gordon JL. Microbial ecology: human gut microbes associated with obesity. *Nature.* 2006;444:1022–1023. DOI: 10.1038/4441022a.
35. Gibiino G, Lopetuso LR, Scalfarri F, Rizzatti G, Binda C, Gasbarrini A. Exploring bacteroidetes: metabolic key points and immunological tricks of our gut commensals. *Dig Liver Dis.* 2018;50:635–639. DOI: 10.1016/j.dld.2018.03.016.
36. Orekhov AN. LDL and foam cell formation as the basis of atherogenesis. *Curr Opin Lipidol.* 2018;29:279–284. DOI: 10.1097/MOL.0000000000000525.
37. Makinen PI, Lappalainen JP, Heinonen SE, Leppanen P, Lahtenvuo MT, Aarnio JV, Heikkila J, Turunen MP, Yla-Herttuala S. Silencing of either SR-A or CD36 reduces atherosclerosis in hyperlipidaemic mice and reveals reciprocal upregulation of these receptors. *Cardiovasc Res.* 2010;88:530–538. DOI: 10.1093/cvr/cvq235.
38. Dai XY, Cai Y, Mao DD, Qi YF, Tang C, Xu Q, Zhu Y, Xu MJ, Wang X. Increased stability of phosphatase and tensin homolog by intermedin leading to scavenger receptor A inhibition of macrophages reduces atherosclerosis in apolipoprotein E-deficient mice. *J Mol Cell Cardiol.* 2012;53:509–520. DOI: 10.1016/j.yjmcc.2012.07.006.
39. Zhu XD, Zhuang Y, Ben JJ, Qian LL, Huang HP, Bai H, Sha JH, He ZG, Chen Q. Caveolae-dependent endocytosis is required for class A macrophage scavenger receptor-mediated apoptosis in macrophages. *J Biol Chem.* 2011;286:8231–8239. DOI: 10.1074/jbc.M110.145888.
40. Ko WK, Lee SH, Kim SJ, Jo MJ, Kumar H, Han IB, Sohn S. Anti-inflammatory effects of ursodeoxycholic acid by lipopolysaccharide-stimulated inflammatory responses in RAW 264.7 macrophages. *PLoS One.* 2017;12:e0180673. DOI: 10.1371/journal.pone.0180673.
41. Thompson PD. What to believe and do about statin-associated adverse effects. *JAMA.* 2016;316:1969–1970. DOI: 10.1001/jama.2016.16557.
42. Thompson PD, Panza G, Zaleski A, Taylor B. Statin-associated side effects. *J Am Coll Cardiol.* 2016;67:2395–2410. DOI: 10.1016/j.jacc.2016.02.071.
43. Marston NA, Kamanu FK, Nordio F, Gurmu Y, Roselli C, Sever PS, Pedersen TR, Keech AC, Wang H, Lira Pineda A, et al. Predicting benefit from evolocumab therapy in patients with atherosclerotic disease using a genetic risk score: results from the FOURIER trial. *Circulation.* 2020;141:616–623. DOI: 10.1161/CIRCULATIONAHA.119.043805.
44. Gürgöze MT, Muller-Hansma AHG, Schreuder MM, Galema-Boers AMH, Boersma E, Roeters van Lennep JE. Adverse events associated with PCSK9 inhibitors: a real-world experience. *Clin Pharmacol Ther.* 2019;105:496–504. DOI: 10.1002/cpt.1193.
45. Lebeau PF, Byun JH, Platko K, Al-Hashimi AA, Lhoták Š, MacDonald ME, Mejia-Benitez A, Prat A, Igodura SA, Trigatti B, et al. Pcsk9 knock-out exacerbates diet-induced non-alcoholic steatohepatitis, fibrosis and liver injury in mice. *JHEP Rep.* 2019;1:418–429. DOI: 10.1016/j.jhepr.2019.10.009.
46. Staels B, Fonseca VA. Bile acids and metabolic regulation: mechanisms and clinical responses to bile acid sequestration. *Diabetes Care.* 2009;32:S237–S245. DOI: 10.2337/dc09-S355.
47. Mueller M, Thorell A, Claudel T, Jha P, Koefeler H, Lackner C, Hoesel B, Fauler G, Stojakovic T, Einarsson C, et al. Ursodeoxycholic acid exerts farnesoid X receptor-antagonistic effects on bile acid and lipid metabolism in morbid obesity. *J Hepatol.* 2015;62:1398–1404. DOI: 10.1016/j.jhep.2014.12.034.
48. Simental-Mendia LE, Simental-Mendia M, Sanchez-Garcia A, Banach M, Serban MC, Cicero AFG, Sahebkar A. Impact of ursodeoxycholic acid on circulating lipid concentrations: a systematic review and meta-analysis of randomized placebo-controlled trials. *Lipids Health Dis.* 2019;18:88. DOI: 10.1186/s12944-019-1041-4.
49. Kotb MA. Molecular mechanisms of ursodeoxycholic acid toxicity & side effects: ursodeoxycholic acid freezes regeneration & induces hibernation mode. *Int J Mol Sci.* 2012;13:8882–8914. DOI: 10.3390/ijms13078882.
50. Singh V, Yeoh BS, Vijay-Kumar M. Gut microbiome as a novel cardiovascular therapeutic target. *Curr Opin Pharmacol.* 2016;27:8–12. DOI: 10.1016/j.coph.2016.01.002.
51. Kazemian N, Mahmoudi M, Halperin F, Wu JC, Pakpour S. Gut microbiota and cardiovascular disease: opportunities and challenges. *Microbiome.* 2020;8:36. DOI: 10.1186/s40168-020-00821-0.
52. Liu B, Zhang Y, Wang R, An Y, Gao W, Bai L, Li Y, Zhao S, Fan J, Liu E. Western diet feeding influences gut microbiota profiles in ApoE knockout mice. *Lipids Health Dis.* 2018;17:159. DOI: 10.1186/s12944-018-0811-8.
53. Cui L, Zhao T, Hu H, Zhang W, Hua X. Association study of gut flora in coronary heart disease through high-throughput sequencing. *Biomed Res Int.* 2017;2017:3796359. DOI: 10.1155/2017/3796359.
54. Van den Bossche L, Hindryckx P, Devisscher L, Devriese S, Van Welden S, Holvoet T, Vilchez-Vargas R, Vital M, Pieper DH, Vanden Bussche J, et al. Ursodeoxycholic acid and its taurine- or glycine-conjugated species reduce colitogenic dysbiosis and equally suppress experimental colitis in mice. *Appl Environ Microbiol.* 2017;83:e02766. DOI: 10.1128/AEM.02766-16.
55. Xu J, Mahowald MA, Ley RE, Lozupone CA, Hamady M, Martens EC, Henrissat B, Coutinho PM, Minx P, Latreille P, et al. Evolution of symbiotic bacteria in the distal human intestine. *PLoS Biol.* 2007;5:e156. DOI: 10.1371/journal.pbio.0050156.
56. Kelly TN, Bazzano LA, Ajami NJ, He H, Zhao J, Petrosino JF, Correa A, He J. Gut microbiome associates with lifetime cardiovascular disease risk profile among Bogalusa Heart Study participants. *Circ Res.* 2016;119:956–964. DOI: 10.1161/CIRCRESAHA.116.309219.
57. Zhang Y, Xu J, Wang X, Ren X, Liu Y. Changes of intestinal bacterial microbiota in coronary heart disease complicated with nonalcoholic fatty liver disease. *BMC Genom.* 2019;20:862. DOI: 10.1186/s12864-019-6251-7.
58. Matziouridou C, Marungruang N, Nguyen TD, Nyman M, Fak F. Lingonberries reduce atherosclerosis in ApoE(-/-) mice in association with altered gut microbiota composition and improved lipid profile. *Mol Nutr Food Res.* 2016;60:1150–1160. DOI: 10.1002/mnfr.201500738.
59. Khan TJ, Ahmed YM, Zamzami MA, Mohamed SA, Khan I, Baotthman OAS, Mehanna MG, Yasir M. Effect of atorvastatin on the gut microbiota of high fat diet-induced hypercholesterolemic rats. *Sci Rep.* 2018;8:662. DOI: 10.1038/s41598-017-19013-2.
60. Li L, Guo WL, Zhang W, Xu JX, Qian M, Bai WD, Zhang YY, Rao PF, Ni L, Lv XC. *Grifola frondosa* polysaccharides ameliorate lipid metabolic disorders and gut microbiota dysbiosis in high-fat diet fed rats. *Food Funct.* 2019;10:2560–2572. DOI: 10.1039/c9fo00075e.
61. Yang T, Santisteban MM, Rodriguez V, Li E, Ahmari N, Carvajal JM, Zadeh M, Gong M, Qi Y, Zubecevic J, et al. Gut dysbiosis is linked to hypertension. *Hypertension.* 2015;65:1331–1340. DOI: 10.1161/HYPERTENSIONAHA.115.05315.
62. O'Connor A, Quizon PM, Albright JE, Lin FT, Bennett BJ. Responsiveness of cardiometabolic-related microbiota to diet is influenced by host genetics. *Mamm Genome.* 2014;25:583–599. DOI: 10.1007/s00335-014-9540-0.
63. Parker BJ, Wearsch PA, Veloo ACM, Rodriguez-Palacios A. The genus *Alistipes*: gut bacteria with emerging implications to inflammation, cancer, and mental health. *Front Immunol.* 2020;11:906. DOI: 10.3389/fimmu.2020.00906.
64. Vieira-Silva S, Falony G, Belda E, Nielsen T, Aron-Wisniewsky J, Chakaroun R, Forslund SK, Assmann K, Valles-Colomer M, Nguyen TTD, et al. Statin therapy is associated with lower prevalence of gut microbiota dysbiosis. *Nature.* 2020;581:310–315. DOI: 10.1038/s41586-020-2269-x.
65. Hugenholtz F, de Vos WM. Mouse models for human intestinal microbiota research: a critical evaluation. *Cell Mol Life Sci.* 2018;75:149–160. DOI: 10.1007/s00018-017-2693-8.
66. Vujkovic-Cvijin I, Sklar J, Jiang L, Natarajan L, Knight R, Belkaid Y. Host variables confound gut microbiota studies of human disease. *Nature.* 2020;587:448–454. DOI: 10.1038/s41586-020-2881-9.
67. Nguyen TL, Vieira-Silva S, Liston A, Raes J. How informative is the mouse for human gut microbiota research? *Dis Model Mech.* 2015;8:1–16. DOI: 10.1242/dmm.017400.

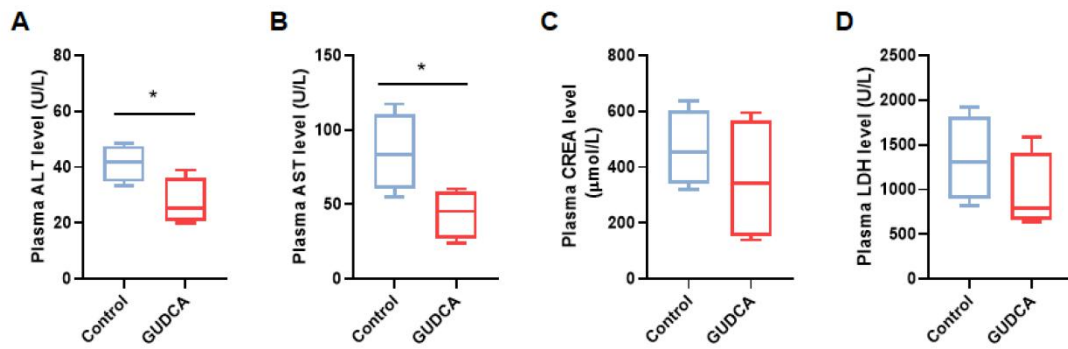
SUPPLEMENTAL MATERIAL

Figure S1. Gene expressions related to intestinal cholesterol excretion.



Relative mRNA levels of ABCG5, ABCG8 and ACAT2 in the ileum of mice. GAPDH mRNA was used as internal control. n= 3 mice per groups. Data are representative of two independent experiments and shown as mean \pm standard error of mean (SEM). Statistical analyses were performed with unpaired two-tailed Student's *t*-test with or without Welch correction, depending on the distribution of these data. * P <0.05, ** P <0.01 and *** P <0.001 versus Control. ABCG5, ATP-binding cassette transporter G5; ABCG8, ATP-binding cassette transporter G8; ACAT2, Acyl-CoA cholesteryl acyl transferases 2

Figure S2. Plasma biochemical indexes.



The levels of (A) alanine aminotransferase (ALT), (B) aspartate aminotransferase (AST), (C) creatinine (CREA) and (D) lactate dehydrogenase (LDH) in plasma. $n=4$ mice per groups. Data are represented as box plots, where the boxes indicate the median and the interquartile ranges and the whiskers show as the minimum and maximum values. Statistical analyses were performed with unpaired two-tailed Student's t -test with or without Welch correction, depending on the distribution of these data. * $P<0.05$, ** $P<0.01$ and *** $P<0.001$ versus Control.